Supplementary Materials for:
Torsional Disorder in Tetraphenyl [3]-Cumulenes: Insight into Excited State Quenching

David Bain, Julia Chang, Yihuan Lai, Thomas Khazanov, Phillip Milner, Andrew Musser

1. Synthesis of Compounds

*1.1 tetraphenyl-[3]-cumulene (**TPC**)*

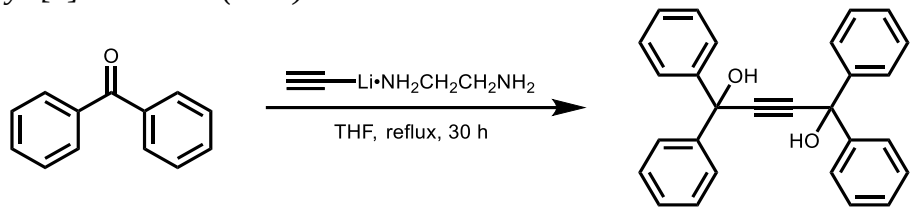

Figure S1. Synthesis of 1,1,4,4,-tetraphenylbut-2-yne-1,4-diol.

Prepared according to the literature procedure [47]. Under a N_2 atmosphere, lithium acetylide ethylenediamine complex (1.38 g, 15.0 mmol, 1.50 equiv.) was added portion-wise to a stirring solution of benzophenone (1.82 g, 10.0 mmol, 1.00 equiv.) dissolved in anhydrous THF (10 mL) in a 50 mL round-bottom flask. The solution was heated to reflux and allowed to stir at reflux for 30 h under N_2. At this time, the reaction mixture was allowed to cool to room temperature and diluted with EtOAc (30 mL). The organic layer was washed with saturated aq. NH_4Cl (30 mL). The layers were separated, and the aqueous layer was extracted with EtOAc (3 × 30 mL). The combined organic extracts were dried over $MgSO_4$ and filtered. The solvent was removed under reduced pressure, and the resulting solid was purified by column chromatography (SiO_2, gradient of 0% → 15% EtOAc in hexanes) to afford 1,1,4,4-tetraphenylbut-2-yne-1,4-diol (1.36 g, 70% yield) as a white solid. ^{1}H NMR (400 MHz, $CDCl_3$): δ 7.61–7.57 (m, 8H), 7.32 (tt, J = 7.4, 1.8 Hz, 8H), 7.28 (tt, J = 7.2, 1.4 Hz, 4H), 2.87 (s, 2H) ppm. This spectrum is consistent with that reported in the literature [47].

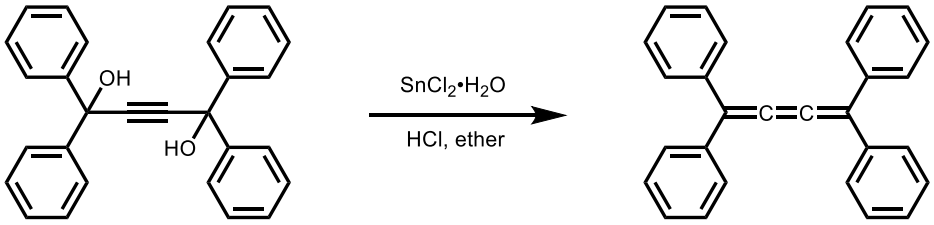

Figure S2. Synthesis of TPC.

Prepared according to the literature procedure [47]. Under a N_2 atmosphere, $SnCl_2 \cdot 2H_2O$ (0.630 g, 3.30 mmol, 1.10 equiv.) was added to a stirred suspension of 1,1,4,4-tetraphenylbut-2-yne-1,4-diol (1.17 g, 3.00 mmol, 1.00 equiv.) in anhydrous Et_2O (20 mL) in a 50 mL 3-neck round-bottom flask. The mixture was cooled to −40 °C using an MeCN/dry ice bath, and HCl (2.00 M in Et_2O, 1.70 mL, 3.40 mmol, 1.13 equiv.) was added via syringe. The reaction mixture was allowed to warm to room temperature and stirred for 14 h at room temperature under N_2. At this time, the yellow heterogeneous mixture was filtered, and the resulting solid was rinsed with deionized water (20 mL) and Et_2O (50 mL) and dried under vacuum to yield **TPC** (0.960 g,

90%) as a yellow solid. ^{1}H NMR (400 MHz, $CDCl_3$): δ 7.57 (d, *J* = 7.2 Hz, 8 H), 7.41–7.32 (m, 12H) ppm; ^{13}C NMR (101 MHz, $CDCl_3$): δ 151.93, 138.72, 129.42, 128.39, 127.94, 122.68 ppm. These spectra are consistent with those reported in the literature [47].

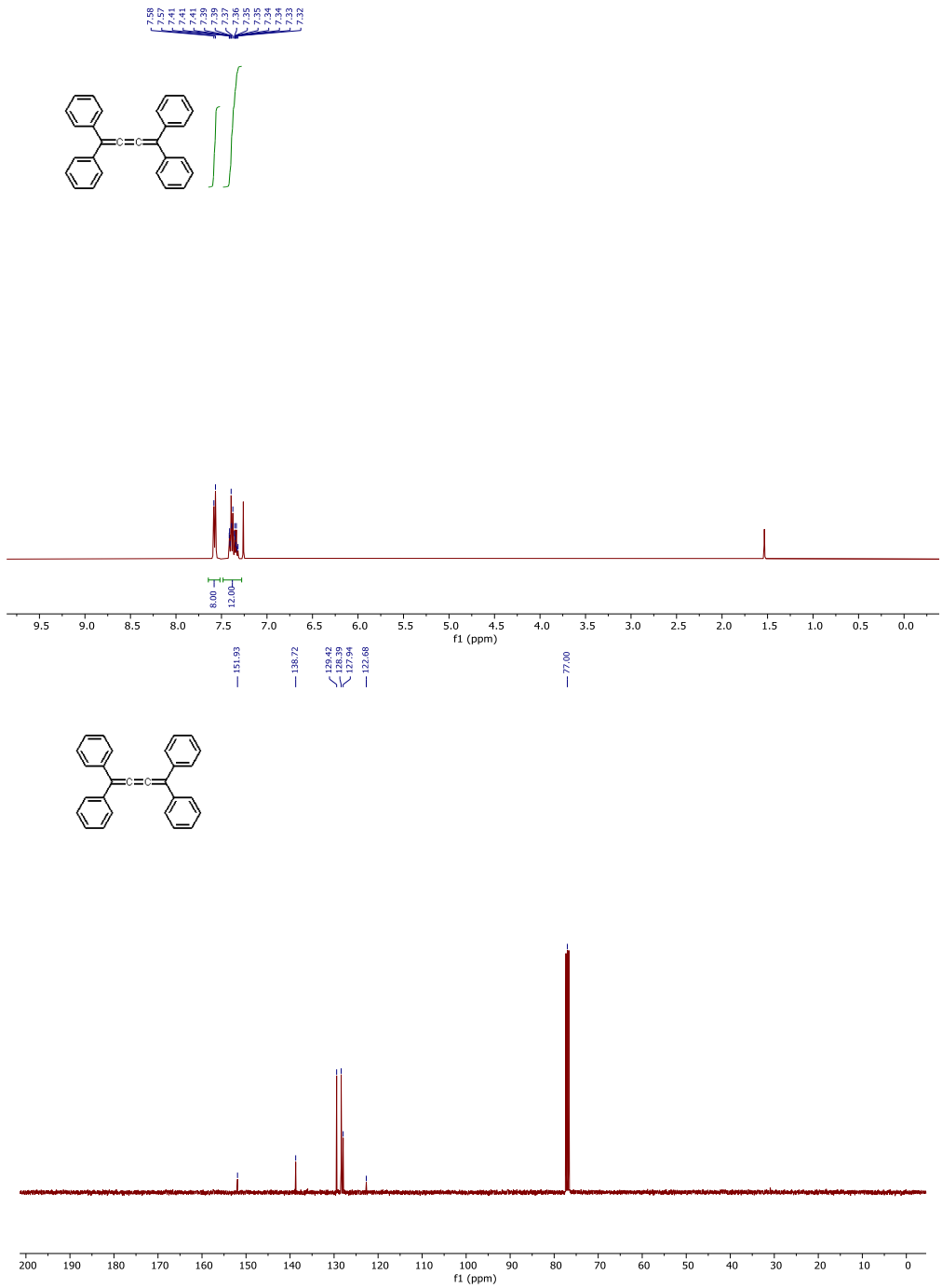

Figure S3. ^{1}H NMR (400 MHz, $CDCl_3$) and ^{13}C NMR (101 MHz, $CDCl_3$) spectra of **TPC**.

*1.2 Bridged version of tetraphenyl-[3]-cumulene (**TPCb**)*

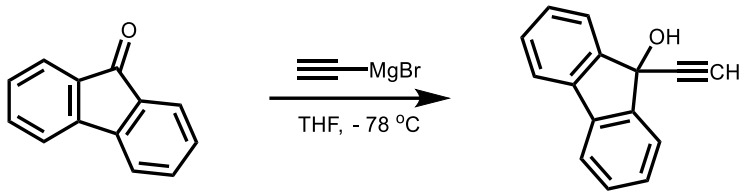

Figure S4. Synthesis of 9-ethynyl-9H-fluoren-9-ol.

Prepared according to the literature procedure [48]. Under a N_2 atmosphere, 9-fluorenone (1.80 g, 10.0 mmol, 1.00 equiv.) was dissolved in 20 mL of anhydrous THF in a 100 mL round-bottom flask. The solution was cooled to −78 °C using an acetone/dry ice bath, and ethynylmagnesium bromide (0.5 M in hexanes, 24.0 mL, 12.0 mmol, 1.20 equiv.) was added dropwise. The solution was allowed to warm to room temperature and stirred for 16 h at room temperature under N_2. At this time, the reaction mixture was quenched with 5% aq. HCl (20 mL), and the layers were separated. The aqueous layer was extracted with Et_2O (2 × 50 mL). The combined organic layers were dried over $MgSO_4$ and filtered. The solvent was removed under reduced pressure, and the resulting solid was purified by column chromatography (SiO_2, gradient of 5% → 35% EtOAc in hexanes) to afford 9-ethynyl-9*H*-fluoren-9-ol (1.16 g, 56%) as a yellow solid. ^{1}H NMR (400 MHz, $CDCl_3$): δ 7.72 (dt, *J* = 7.6 Hz, 0.8 Hz, 2H), 7.64 (dt, *J* = 7.6 Hz, 0.8 Hz, 2H), 7.41 (tdd, *J* = 7.6 Hz, 1.2 Hz, 0.8 Hz, 2H), 7.37 (tdd, *J* = 7.6 Hz, 1.2 Hz, 0.8 Hz, 2H), 2.48 (s, 1H). This spectrum is consistent with that reported in the literature [48].

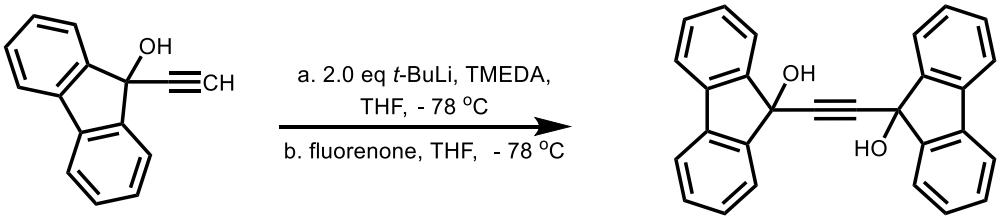

Figure S5. Synthesis of 9-(2-(9-Hydroxy-9H-fluoren-9-yl)ethynyl)-9H-fluoren-9-ol.

Prepared according to the literature procedure [48]. Under a N_2 atmosphere, 9-ethynyl-9*H*-fluoren-9-ol (1.16 g, 5.60 mmol, 1.20 equiv.) was dissolved in anhydrous THF (15 mL) under a N_2 atmosphere in a 100 mL 3-neck round-bottom flask. The solution was cooled to −78 °C using an acetone/dry ice bath. *t*-butyllithium (1.5 M in hexanes, 7.5 mL, 11.2 mmol, 2.00 equiv.) was added dropwise, followed by dropwise addition of anhydrous tetramethylenediamine (TMEDA, 8.5 mL, 56 mmol, 10.00 equiv.). The reaction mixture was stirred at −78 °C for 1 h. At this time, 9-fluorenone (0.85 g, 4.70 mmol, 1.00 equiv.) dissolved in anhydrous THF (30 mL) was added via syringe. The solution was allowed to warm to room temperature and stirred for 20 h at room temperature under N_2. At this time, the reaction mixture was quenched with saturated aq. NH_4Cl (30 mL), and the aqueous layer was extracted with Et_2O (3 × 30 mL). The combined organic layers were washed with 5% aq. HCl (2 × 20 mL), deionized water (20 mL), and brine (30 mL), dried over $MgSO_4$, filtered, and concentrated under reduced pressure. The resulting solid was purified by column chromatography (SiO_2, gradient of 10% → 70% EtOAc in hexanes) to yield 9-(2-(9-Hydroxy-9*H*-fluoren-9-yl)ethynyl)-9*H*-fluoren-9-ol (0.650 g, 72%) as a white solid. ^{1}H NMR (400 MHz, acetone-d_6): δ 7.72 (d, *J* = 7.8 Hz, 4H), 7.64 (d, *J* = 6.9 Hz,

4H), 7.38 (t, *J* = 6.9 Hz, 4H), 7.32 (t, *J* = 7.2 Hz, 4H), 5.50 (s, 2H). This spectrum is consistent with that reported in the literature [48].

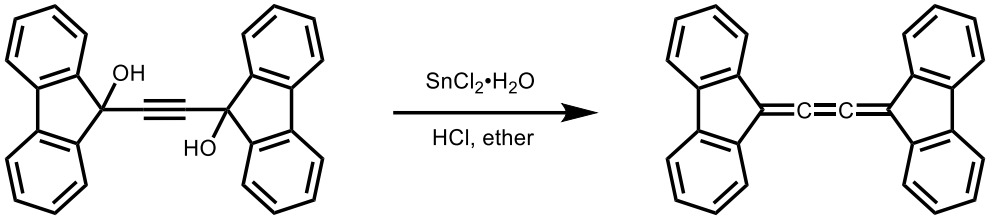

Figure S6. Synthesis of **TPCb**.

Prepared according to the literature procedure [48]. Under a N_2 atmosphere, $SnCl_2 \cdot 2H_2O$ (0.372 g, 1.65 mmol, 1.10 equiv.) was added to a stirred suspension of 9-(2-(9-hydroxy-9*H*-fluoren-9-yl)ethynyl)-9*H*-fluoren-9-ol (0.58 g, 1.50 mmol, 1.00 equiv.) in anhydrous Et_2O (20 mL) in a 50 mL 3-neck round-bottom flask. The mixture was cooled to −40 °C using an MeCN/dry ice bath, and HCl (2.00 M in Et_2O, 0.850 mL, 1.70 mmol, 1.13 equiv.) was added to the mixture via syringe. The reaction mixture was allowed to warm to room temperature and stirred for 14 h at room temperature under N_2. The red heterogeneous mixture was filtered, and the resulting solid was rinsed with deinoized water (20 mL) and Et_2O (50 mL) and dried under vacuum to yield **TPCb** (0.496 g, 94%) as a red solid. ^{1}H NMR (400 MHz, CD_2Cl_2): δ 7.89–7.87 (m, 4 H), 7.75–7.73 (m, 4H), 7.44–7.37 (m, 8 H). This spectrum is consistent with that reported in the literature [48]. **TPCb** exhibits poor solubility in all tested organic solvents, which precluded us from collecting a ^{13}C NMR spectrum of it.

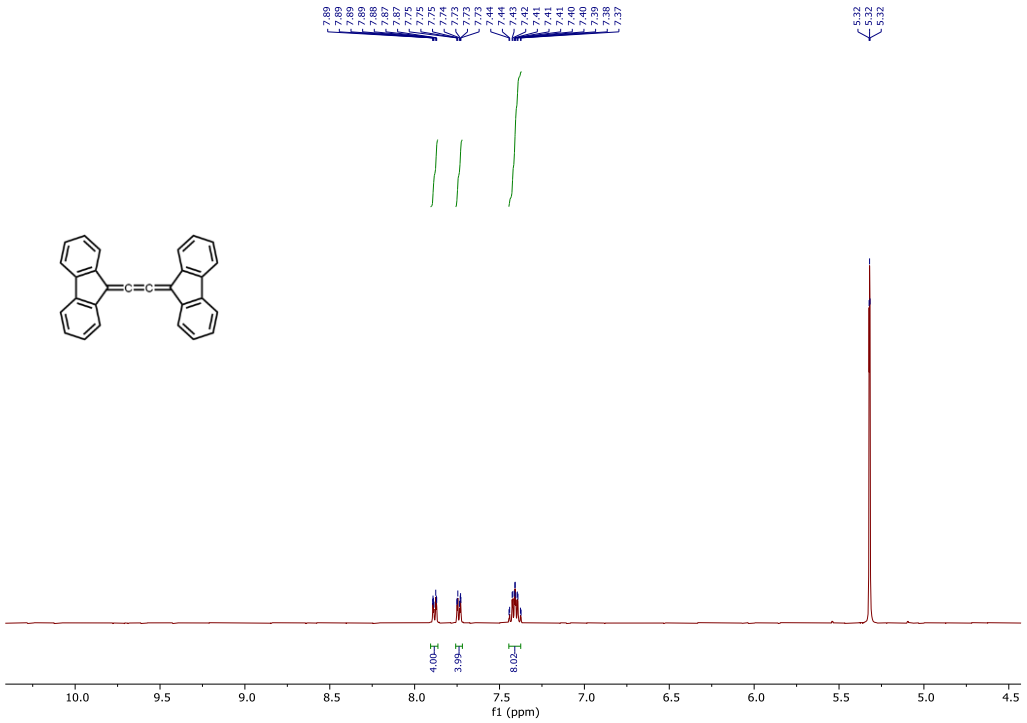

Figure S7. ^{1}H NMR (400 MHz, $CDCl_3$) spectra of **TPCb**.

2. Computational Details

Representative geometry optimization, frequency, and single-point calculation input for ORCA 5.0.4:

```
!B3LYP RIJCOSX def2-TZVP(-f) AutoAux
!NormalPrint Opt Freq
!PrintBasis UNO UCO MOREAD

%moinp "cumulene_opt2.gbw"

%maxcore 5000

%output print[p_mos] 1 end
%SCF   Directresetfreq 1
       DIIS MaxEq 15
          end
       Shift Shift 0.5
            Erroff 0.1
            end
       MaxIter 1000
       end

* xyzfile 0 1 sample.xyz
```

Representative TDDFT input:

```
!B3LYP RIJCOSX def2-TZVP(-f) AutoAux
!NormalPrint
!UNO UCO MOREAD

%moinp "cumulene_opt_freq.gbw"

%maxcore 5000

%TDDFT NROOTS 10
END

* xyzfile 0 1 sample.xyz
```

2.1 TPC calculations

Table S1. Optimized TPC geometry on the S_0 potential energy surface.

C	1.28481585116900	-0.00000996778279	0.00000339269208
C	-0.05411199147144	-0.00001009927105	0.00001061464675
C	2.53576544999558	-0.00000846302283	-0.00000322347002
C	3.87468731747940	-0.00000441268786	-0.00001130727603
C	-0.78190126941377	1.28010981481203	0.15684975814761

C	-0.24652755281822	2.31670021469786	0.93424808902147
C	-0.90242147636262	3.53362781984392	1.04872797292893
C	-2.10621997573921	3.74764489742124	0.38437987197488
C	-2.64779494434039	2.73009204736568	-0.39375725309084
C	-1.99683625733054	1.50891715818928	-0.50432846894676
H	0.68694824732439	2.15441447159612	1.45770295949784
H	-0.47470068636784	4.31672200075052	1.66284825088680
H	-2.61831794285044	4.69767869156502	0.47363686149989
H	-3.57950005230757	2.88886130308051	-0.92300171629719
H	-2.42214325579098	0.73103145732021	-1.12449129400670
C	-0.78190500602423	-1.28012701308601	-0.15683188770515
C	-1.99685112300650	-1.50892439328375	0.50432949001155
C	-2.64781425654944	-2.73009681350491	0.39375634496450
C	-2.10623118762389	-3.74765815606171	-0.38436387678849
C	-0.90242133960129	-3.53365137020104	-1.04869492531384
C	-0.24652399205650	-2.31672575569316	-0.93421431274834
H	-2.42216416855202	-0.73103245036313	1.12448014367518
H	-3.57952838457060	-2.88885769657354	0.92298742020586
H	-2.61833214234999	-4.69769025587190	-0.47362217122668
H	-0.47469447392214	-4.31675240567879	-1.66280219229751
H	0.68696105217909	-2.15444856347898	-1.45765540373966
C	4.60274574898024	1.28715382335399	0.07723435280690
C	4.06825944346690	2.44721739397645	-0.50055794200007
C	4.72480659243925	3.66442153154677	-0.39266265122034
C	5.92868180641741	3.75387083068324	0.29944600457015
C	6.46918677314006	2.61241897873680	0.88183448272092
C	5.81736142650051	1.39178908267733	0.76960885015127
C	4.60275372469508	-1.28715871228846	-0.07724315896975
C	5.81737318702416	-1.39179218060396	-0.76961137117634
C	6.46920602316241	-2.61241912141709	-0.88182475624366
C	4.06827227850687	-2.44722082341545	0.50055666166952
C	4.72482725160164	-3.66442185597936	0.39267390582590
C	5.92870631447443	-3.75386942173588	-0.29942836802329
H	6.24178512448165	0.51430894669921	1.23919436391963
H	6.44118268779355	4.70418566536954	0.38308645441651
H	7.40088749608931	2.67259414969611	1.43115086658879
H	3.13501964206070	2.38225147283889	-1.04506928192911
H	4.29759384546326	4.54595117712879	-0.85492871269662
H	3.13502918792082	-2.38225654103088	1.04506276412083
H	4.29761792311433	-4.54595037664044	0.85494529868415
H	6.44121324219850	-4.70418182602314	-0.38305928187561
H	6.24179353911807	-0.51431321544866	-1.23920199506412
H	7.40090937505298	-2.67259303740474	-1.43113687332177

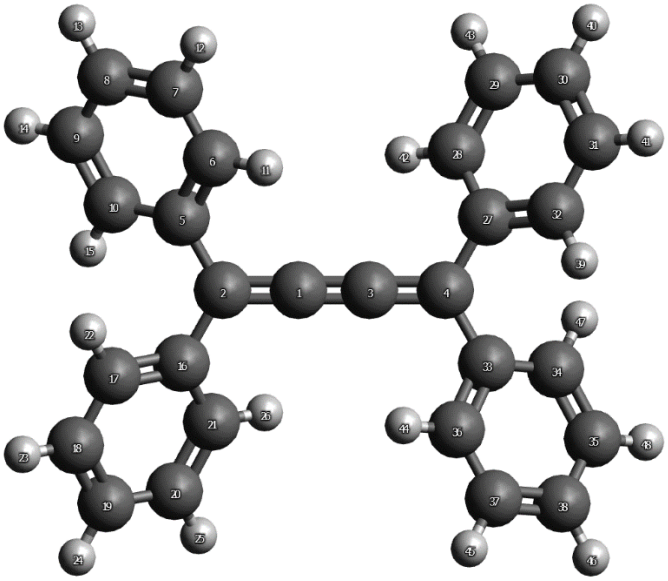

Figure S8. Visualization of the S_0 TPC structure from Table S1.

Table S2. Definition of phenyl group torsion angles for TPC based on Figure S8.

Torsion angle	Atoms	At optimized geometry
α	1-2-5-6	-32.37°
β	3-4-27-28	-32.42°
γ	3-4-33-36	-32.41°
δ	1-2-16-21	-32.37°

Table S3. TDDFT first and second vertical transition energies for TPC as all phenyl groups are rotated symmetrically by the same amount (α=β=γ=δ).

Torsion angle (all)	1st transition wavelength (nm)	1st transition oscillator strength	2nd transition wavelength (nm)	2nd transition oscillator strength
0°	448.7	1.139415866	344.0	0.003465079
-5°	444.7	1.166376959	340.9	0.000387148
-10°	437.6	1.203100633	336.0	0.001688787
-15°	428.9	1.237414740	332.2	0.010309042
-20°	419.9	1.262311940	329.7	0.020318207
-25°	411.1	1.274121172	328.0	0.028867464
-32°	398.3	1.261978267	325.7	0.040591558
-45°	376.0	1.136220486	320.3	0.067977561

Table S4. TDDFT first and second vertical transition energies for TPC as one phenyl group is rotated (α) and the others are fixed at the optimized value of ~32°.

Torsion angle (α)	1st transition wavelength (nm)	1st transition oscillator strength	2nd transition wavelength (nm)	2nd transition oscillator strength
0°	408.0	1.248634936	331.3	0.024361449

-5°	407.3	1.254264086	329.9	0.026786446
-10°	406.2	1.259555729	328.7	0.029583555
-15°	404.8	1.263706390	327.8	0.032404387
-20°	403.2	1.266083892	327.0	0.035057668
-25°	401.3	1.266243178	326.4	0.037445459
-32°	398.3	1.261978267	325.7	0.040591558
-45°	392.5	1.237405598	324.8	0.046753135
-60°	384.7	1.194550284	324.4	0.062412894
-75°	376.2	1.168384833	325.7	0.088346415
-90°	370.1	1.195774779	329.5	0.074403029

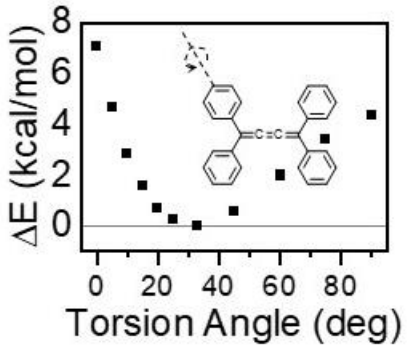

Figure S9. Ground state potential energy curve for rotation of one phenyl group (torsion angle α) on TPC as the others are fixed at the optimized value of ~32°.

Table S5. TDDFT first vertical transition energies for TPC as cumulene twist angle is varied. All other angles are held constant. Twist angle is defined as the dihedral angle between atoms 5, 16, 27, and 33.

Twist angle	1st transition wavelength (nm)	1st transition oscillator strength
-15°	422.5	1.003696624
-10°	412.4	1.085299663
-5°	405.0	1.159600532
0°	400.2	1.225205964
5°	398.1	1.270558304
10°	398.8	1.287273320
15°	402.5	1.265461404

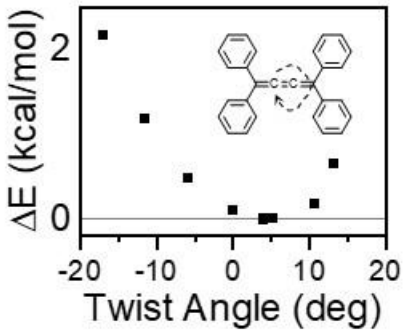

Figure S10. Ground state potential energy curve for cumulene bond twisting in TPC.

2.2 TPC excited state calculations and additional discussion

Table S6. Optimized TPC geometry on the S_1 potential energy surface.

C	1.27662525428259	-0.00002467122801	0.00001646039038
C	-0.07815170731205	-0.00000403105454	0.00001543558116
C	2.53819447022175	-0.00002659869104	0.00000683421461
C	3.89290235491053	-0.00001007910155	0.00001309859109
C	-0.78870841318633	1.01108015702652	-0.79961940436019
C	-0.18466991180382	2.25112554393495	-1.07867374928933
C	-0.81325490477427	3.19113611131765	-1.87840548957059
C	-2.06066425694626	2.92004018984448	-2.43491031815931
C	-2.66861275536340	1.69377267985244	-2.18083812945128
C	-2.04709486475076	0.75238591701278	-1.37442807080863
H	0.78486618938365	2.46884869525809	-0.64911953966504
H	-0.32954483042390	4.14163009588358	-2.06849328893370
H	-2.55055113967836	3.65319509829206	-3.06337726560540
H	-3.63073355048053	1.46470142424484	-2.62309192388029
H	-2.52109249871603	-0.20595021909119	-1.21250103134687
C	-0.78872804424092	-1.01109377480840	0.79962919039546
C	-2.04708585594422	-0.75236953686369	1.37448667232621
C	-2.66861578267081	-1.69376168177188	2.18088129873529
C	-2.06070900536264	-2.92006421261962	2.43488527244651
C	-0.81333057281376	-3.19119131722202	1.87832698560711
C	-0.18473183163662	-2.25117437720225	1.07861275237846
H	-2.52104785553480	0.20599316109478	1.21261161356389
H	-3.63071251453595	-1.46466837322626	2.62317588257097
H	-2.55060528063682	-3.65322320144753	3.06334002708939
H	-0.32965561351595	-4.14171427868084	2.06835953708370
H	0.78477801212010	-2.46892216655698	0.64901174324393
C	4.60527231571871	0.84809682957571	0.96976999782858
C	4.00474549133612	2.01873829192639	1.46923075896546

C	4.63852271565538	2.79918432974806	2.42196294716232
C	5.88734934498495	2.43074811943952	2.91591455556480
C	6.49082320338407	1.26806622120417	2.44496653368296
C	5.86415981568292	0.48756974291075	1.48545052554346
C	4.60529281148255	-0.84810301765760	-0.96974457975498
C	5.86413973423205	-0.48751078976619	-1.48547653530217
C	6.49082160127864	-1.26799655668450	-2.44498906496353
C	4.00482256787304	-2.01879607267585	-1.46914928543699
C	4.63861863446477	-2.79923140920043	-2.42187861186496
C	5.88740553524043	-2.43073094411271	-2.91588186161790
H	6.33507438633155	-0.42718343351430	1.15280552629929
H	6.38163016457196	3.03915052083499	3.66290810206162
H	7.45374597122312	0.96150541308526	2.83549894749325
H	3.03456029863053	2.31210307914274	1.08893265491820
H	4.15808287923209	3.70139272129681	2.78078619562213
H	3.03467101635424	-2.31221250169676	-1.08880538236104
H	4.15822570789554	-3.70148253158628	-2.78065729968724
H	6.38170126596186	-3.03912572722900	-3.66287179462056
H	6.33500622015911	0.42728207791722	-1.15287206418578
H	7.45371230051583	-0.96138691635432	-2.83556210829443

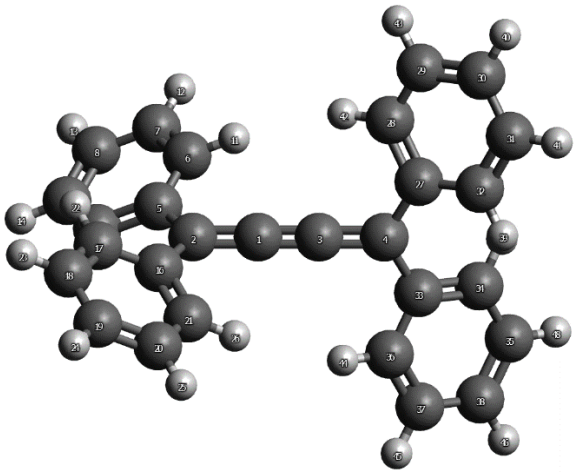

Figure S11. Visualization of the S_1 TPC structure from Table S1.

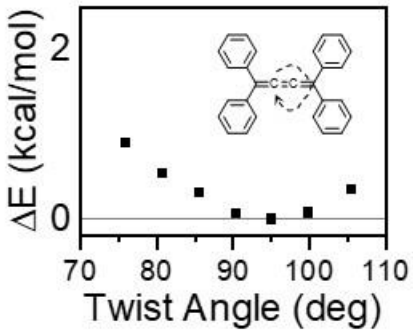

Figure S12. Excited state potential energy curve for cumulene bond twisting in TPC. Twist angle is defined similarly to the ground state as the dihedral angle between atoms 5, 16, 27, and 33.

Based on literature and our calculations, phenyl torsion and cumulene twisting are both possible in the ground and excited states, although the extent of phenyl torsion is expected to have a much more pronounced effect on the energetics and subsequent excited state dynamics than cumulene twisting.

Firstly, cumulenes are generally accepted to be rigid molecules, and literature discussing twisting of the cumulene axis is scarce. One study achieves cis-trans isomerization by applying an electric field and another achieves it through photoexcitation [30,45]. Without any external perturbation to the system, though, the cumulene bond will not fully twist at room temperature. In the excited state, on the other hand, the cumulene axis will preferentially twist by 90°. This is supported by our calculated geometries in on S_0 and S_1 and by our potential energy curves (Figures S8, S10-S12). Since the cumulene twist angle is near 0° in the ground state, this makes our TA measurements on TPCb quite striking. When prepared in a solid-state polymer matrix where cumulene twisting is hindered, we observe nearly identical excited state dynamics to that of a dilute solution measurement where cumulene twisting is easily accessible (Figures 3 and 4). This is in contrast to the several orders of magnitude change in lifetime seen in TPC where phenyl torsion is also enabled. Ultimately, while cumulene twisting will occur in the excited state of TPCb and TPC, it must not be the driver of the quenching mechanism. We characterize the cumulene twisting more carefully by tracking the S_1 PIA redshift over time in solution as discussed in text and shown in Figure S22.

While there exist a few studies investigating cumulene twisting under external perturbations, there are no comparable studies investigating phenyl torsion, to the best of our knowledge. Looking more closely at our potential energy curves for phenyl torsion and cumulene twisting, we find a comparable but slightly smaller change in total energy as phenyl torsion occurs vs cumulene twisting by the same degree, i.e. that motion is energetically more accessible. In addition, our calculations were performed by either varying one phenyl group or all of them symmetrically, while in reality all four phenyl groups can rotate independently, giving rise to a much higher density of phenyl-torsion states. Thus, we ultimately expect phenyl torsion to be the motion primarily responsible for disorder in the ground state with a smaller contribution coming from cumulene twisting. This is in line with our TA measurements that

show stretched exponential decay in a polymer matrix of TPC but only single exponential decay in TPCb (see main text).

2.2 TPCb calculations

Table S7. Optimized TPCb geometry on the S_0 potential energy surface.

C	1.34096071015158	0.00001873354824	0.00000557282785
C	0.00360960073093	0.00001400734312	0.00000055900396
C	2.58891459079045	0.00001907204420	0.00001205807808
C	3.92626652464068	0.00001345921980	0.00001988934562
C	-0.87664900064228	1.17037187545426	0.09727433250417
C	-0.57550860059263	2.52137292738448	0.20930596314006
C	-1.62088631171475	3.43723576299329	0.28442128465112
C	-2.94687393566331	3.00561976836157	0.24772342236600
C	-3.25499082512155	1.65068742662407	0.13553781892094
C	-2.21906337683976	0.73080109732450	0.06043979664148
H	0.45417917770188	2.85570321057485	0.23707054226801
H	-1.40386636858654	4.49443452859279	0.37185910170424
H	-3.74707986012171	3.73291553291435	0.30695182853640
H	-4.28926896857888	1.32961118352892	0.10790271393357
C	-0.87663503162606	-1.17035334477036	-0.09728535156610
C	-2.21905471385972	-0.73079870964118	-0.06046119514718
C	-3.25497100847772	-1.65069623789255	-0.13557610403764
C	-2.94683762867448	-3.00562457156608	-0.24776439248067
C	-1.62084447939124	-3.43722488246830	-0.28445251389395
C	-0.57547821682188	-2.52135017636868	-0.20932340564034
H	-4.28925294179001	-1.32963159677003	-0.10794871637854
H	-3.74703447822908	-3.73292954644031	-0.30700223606679
H	-1.40381100565977	-4.49442053887441	-0.37189431367862
H	0.45421383764068	-2.85566852121108	-0.23707624418709
C	4.80652223022677	1.17044264743116	0.09647395356330
C	4.50539474109078	2.52152233673018	0.20759840878982
C	5.55078575029487	3.43742365077954	0.28207353088197
C	6.87677058306085	3.00577635754997	0.24565800952337
C	7.18487564521952	1.65076325845418	0.13440914806800
C	6.14893454491958	0.73084077997322	0.05995429545320
C	4.80650688294616	-1.17042785947570	-0.09642373884108
C	6.14892495210435	-0.73084488847936	-0.05989585382584
C	7.18485407249125	-1.65078087728432	-0.13435041559964
C	4.50536158911083	-2.52150323677805	-0.20755282820544
C	5.55074032057859	-3.43741850711106	-0.28202603714646
C	6.87673106901709	-3.00578949640226	-0.24560301060524
H	7.67697947907429	3.73311246828760	0.30434510347178
H	8.21914905919415	1.32965547050467	0.10697770077283
H	3.47571347469080	2.85588701789847	0.23516903769232

H	5.33377371774769	4.49468290726968	0.36879988841172
H	3.47567592350173	-2.85585406708047	-0.23512956565378
H	5.33371395892446	-4.49467430626560	-0.36875872617717
H	7.67693017083464	-3.73313671779545	-0.30428673868099
H	8.21913151390672	-1.32968690901187	-0.10691272073724

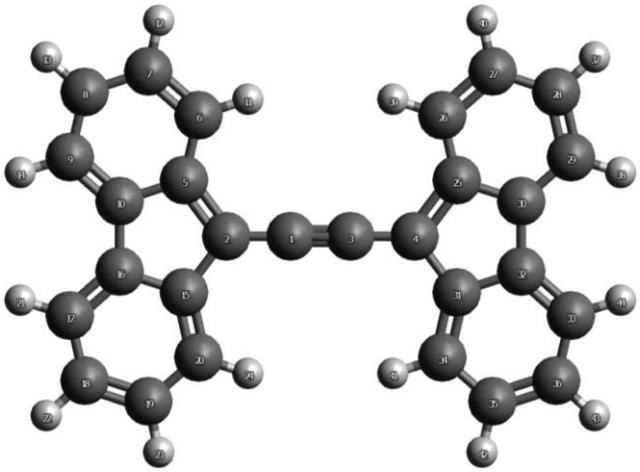

Figure S13. Visualization of the S_0 TPCb structure from Table S7.

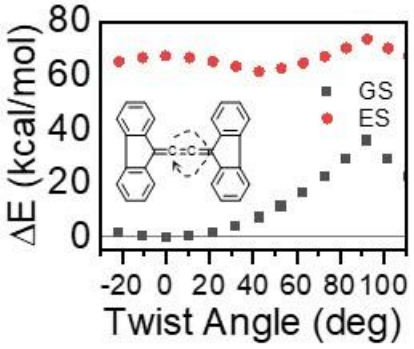

Figure S14. Ground state and excited state potential energy curves for cumulene bond twisting in TPCb. Twist angle is defined equivalently to TPC.

3. Additional Spectroscopic Measurements

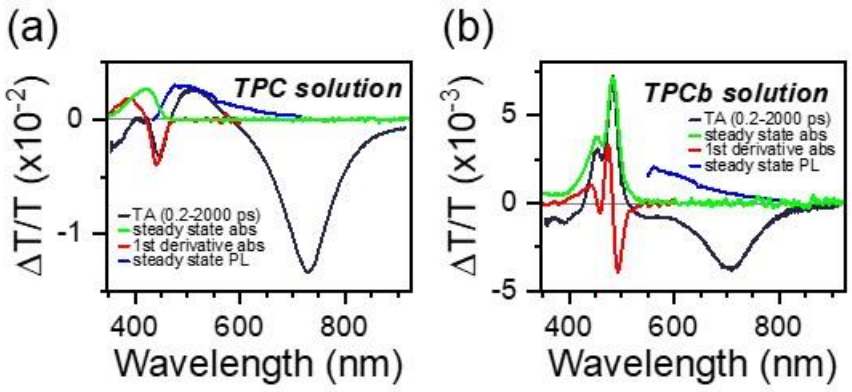

Figure S15. Comparison of time averaged TA spectra for 0.01 mg/mL TPC (a) and TPCb (b) in toluene along with their absorbance, first derivative of absorbance, and PL spectra. Although by eye only the TPC matrix sample is emissive (Figure 5b), we can still resolve weak PL from TPC and TPCb in solution using a sensitive ICCD detector. Because the PL is weak, the signal is noisy. In addition, the high-energy edge of the TPCb PL spectrum is distorted from placing a long pass filter to block pump scatter.

Table S8. Extracted time constants from exponential fitting of TPC solution and matrix. Time constants are in units of picoseconds and amplitudes are given in parentheses.

	solution		matrix	
	440-450 nm	670-750 nm	440-450 nm	670-750 nm
τ1	0.54 (-0.87)	0.13 (-0.25)	0.30 (-0.33)	-
τ2	2.7 (1.6)	2.8 (1.1)	240 (1.4) (β=0.38)	800 (1.1) (β=0.42)
τ3	55 (0.03)	-	-	-

Table S9. Extracted time constants from exponential fitting of TPCb solution and matrix. Time constants are in units of picoseconds and amplitudes are given in parentheses.

	solution		matrix	
	440-490 nm	670-750 nm	440-450 nm	670-750 nm
τ1	-	0.38 (-0.12)	-	-
τ2	13 (1.0)	11 (1.1)	20 (1.0)	17 (0.99)

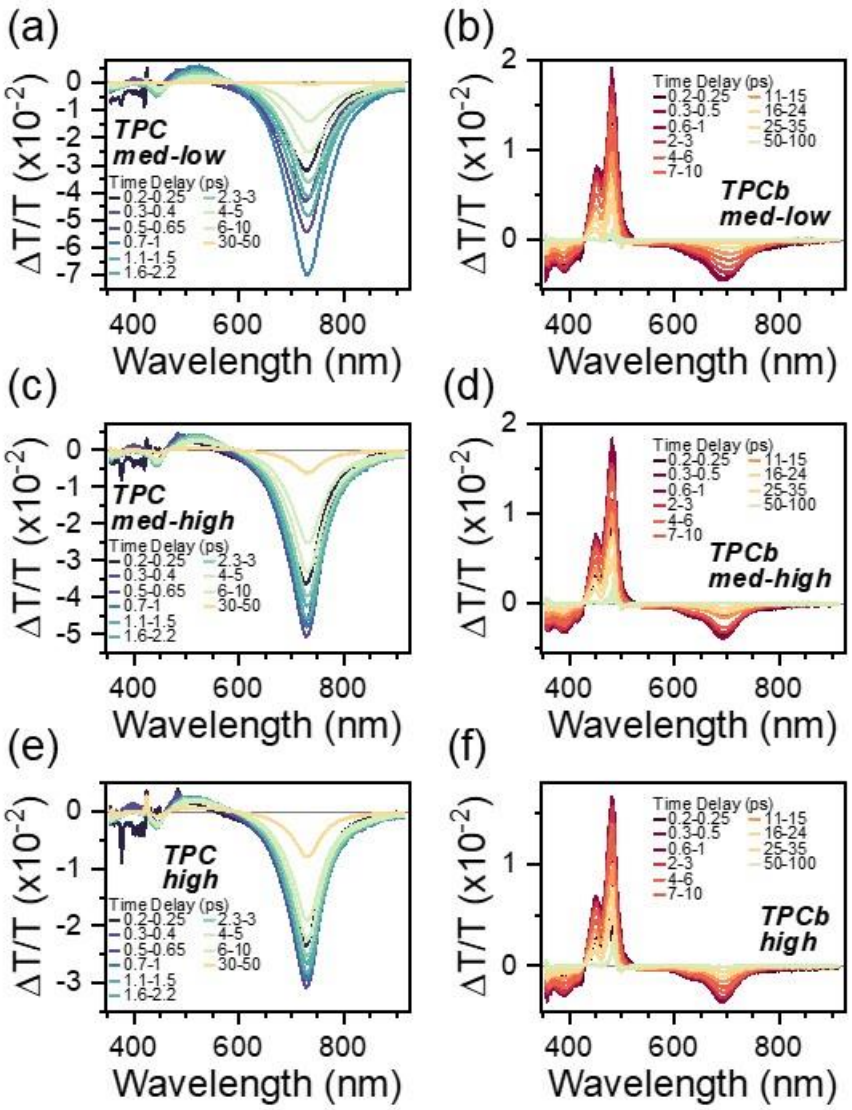

Figure S16. Full viscosity dependent TA spectra for TPC and TPCb. Samples of low, medium-low, medium-high, and high viscosity were measured and compared with polymer matrix data in Figure 4. The low viscosity samples correspond to measurements in pure toluene already presented in Figures 2 and 3, so only the remaining three samples' TA spectra are presented here.

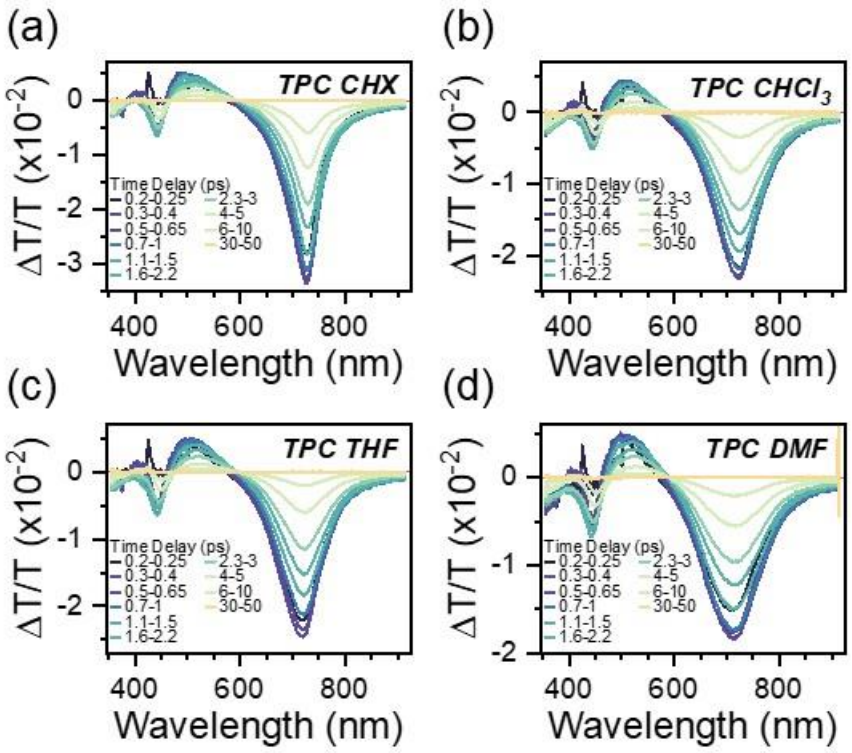

Figure S17. TA spectra for TPC prepared in various solvents. Toluene data is presented in Figure 2.

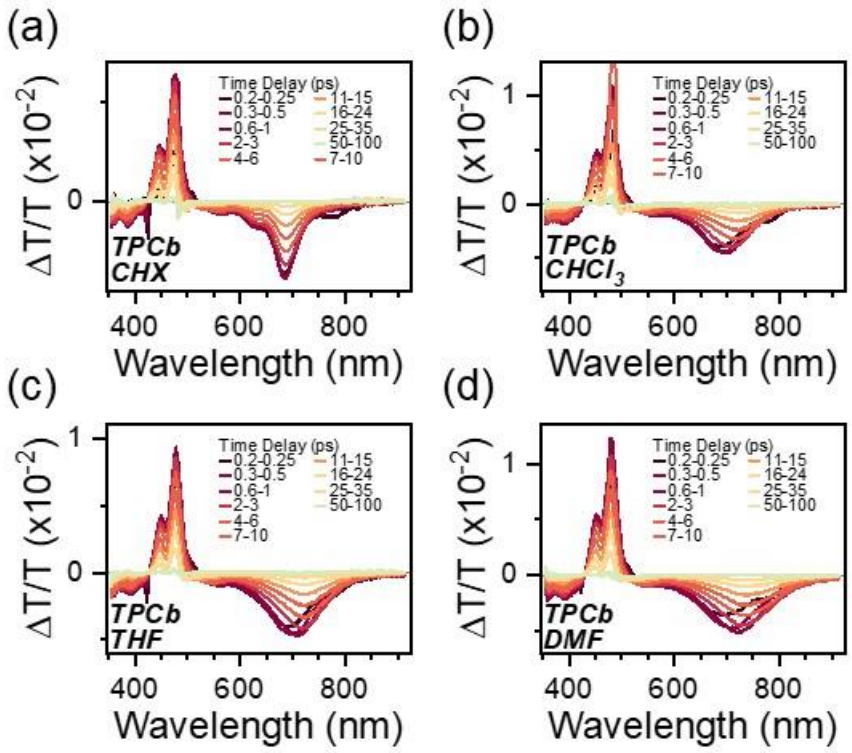

Figure S18. TA spectra for TPCb prepared in various solvents. Toluene data is presented in Figure 3.

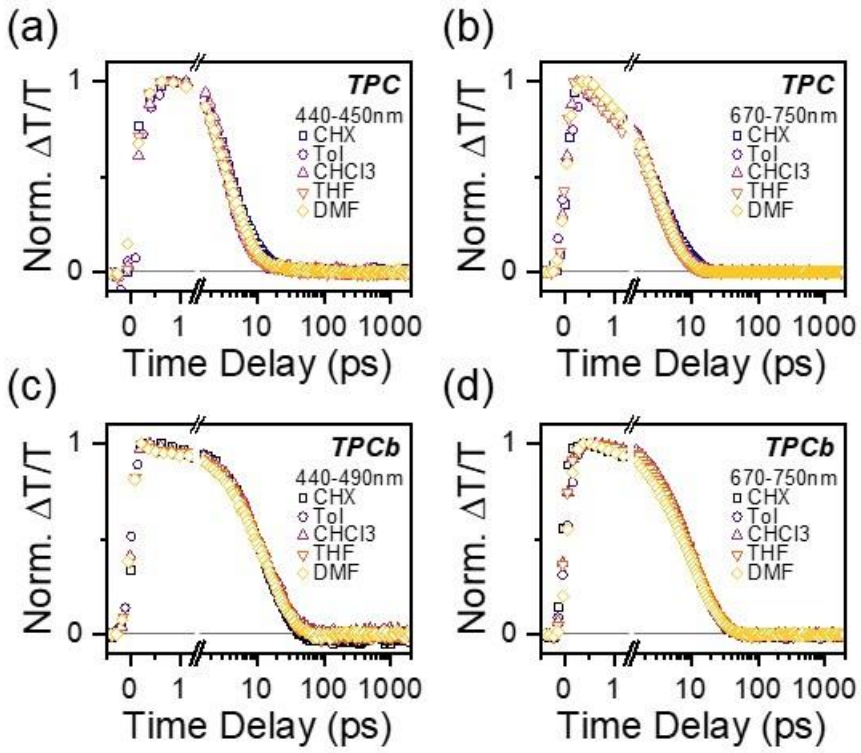

Figure S19. Representative kinetics extracted from solvent dependent TA data. For TPC, the GSA* feature is tracked in (a) and 730 nm PIA is tracked in (b) by integrating over the indicated wavelength ranges. For TPCb, the GSB feature is tracked in (c) and 710 nm PIA is tracked in (d) by integrating over the indicated wavelength ranges.

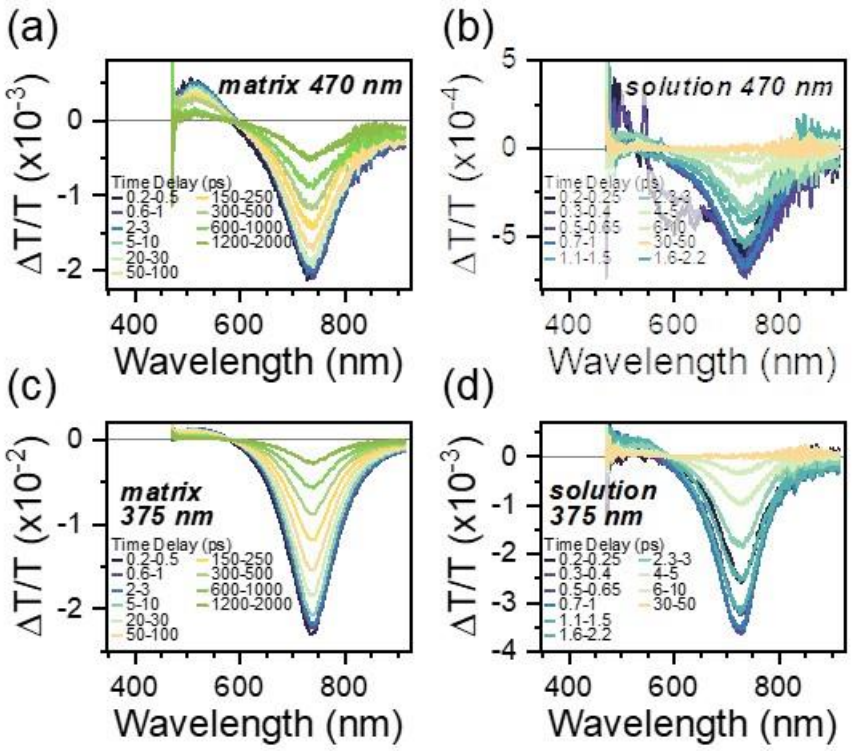

Figure S20. TA data for TPC under red- (a and b) and blue-edge (c and d) excitation. 470 nm was used for red-edge excitation and 375 nm for blue-edge excitation. Ultraviolet probe data was not collected and spliced like in all other TA measurements due to low signal levels and high noise in these nonresonant excitation schemes (see Materials and Methods section for experimental details). Consequently, the data only extends down to 470 nm and GSA* feature is absent. Data is presented for TPC both as a polymer matrix (a and c) and in dilute solution of toluene (b and d).

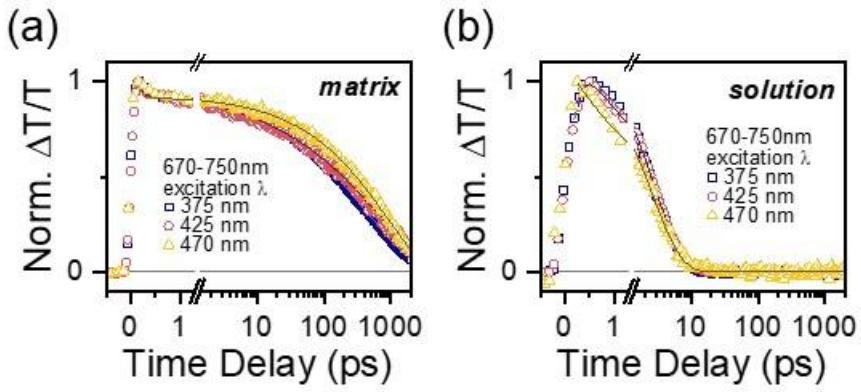

Figure S21. 730 nm kinetics for TPC matrix and dilute solution (b) under red- and blue-edge excitation. Kinetics were extracted by integrating over the indicated wavelength range and are also compared with resonant excitation from Figure 2.

Table S10. Extracted time constants from exponential fitting of TPC under red- and blue-edge excitation. Resonant excitation data from Table 7 is duplicated here for easy comparison.

	matrix			solution		
	blue-edge	resonant	red-edge	blue-edge	resonant	red-edge
τ1	-	-	-	0.21 (-0.43)	0.13 (-0.25)	-
τ2	400 (0.96) (β=0.52)	800 (1.1) (β=0.42)	970 (1.0) (β=0.56)	2.6 (1.2)	2.8 (1.1)	2.7 (1.0)

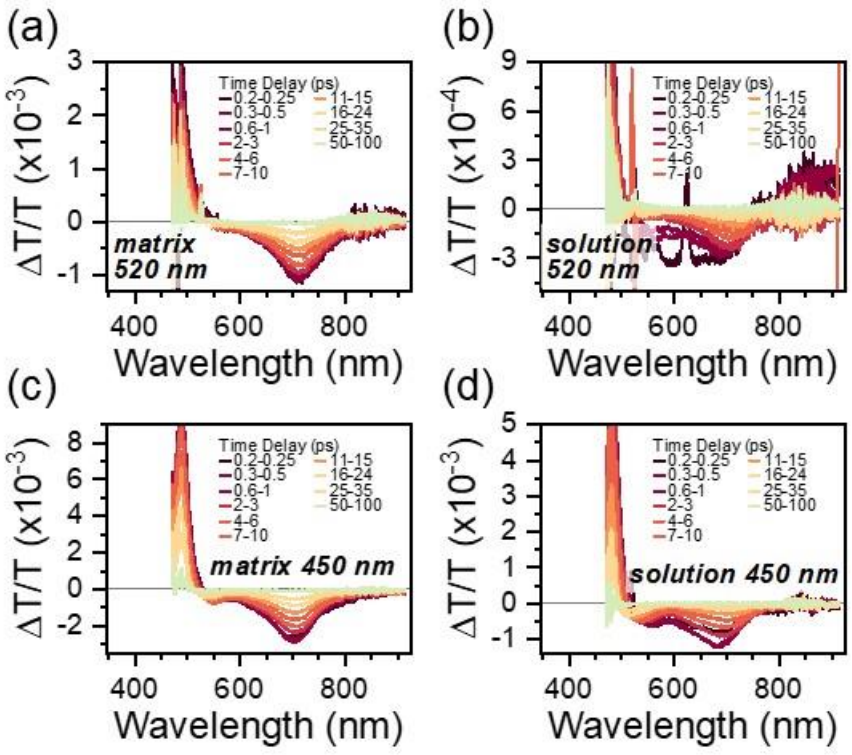

Figure S22. TA data for TPCb under red- (a and b) and blue-edge (c and d) excitation. 520 nm was used for red-edge excitation and 450 nm for blue-edge excitation. Ultraviolet probe data was not collected and spliced like in all other TA measurements due to low signal levels and high noise in these nonresonant excitation schemes (see Materials and Methods section for experimental details). Consequently, the data only extends down to 470 nm and GSB feature is cropped. Data is presented for TPCb both as a polymer matrix (a and c) and in dilute solution of toluene (b and d).

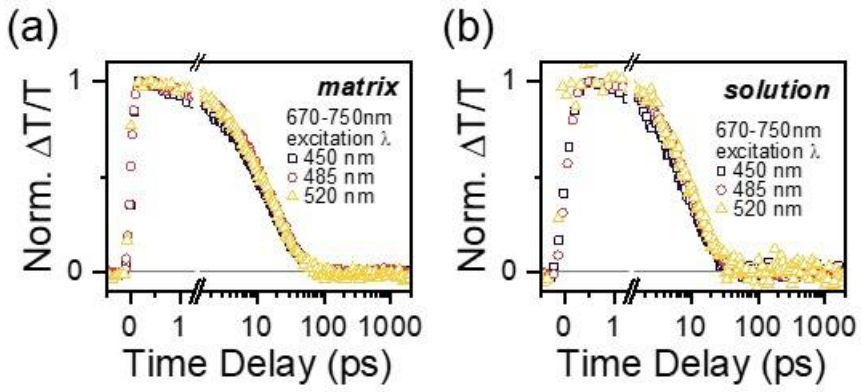

Figure S23. 710 nm kinetics for TPC matrix and dilute solution (b) under red- and blue-edge excitation. Kinetics were extracted by integrating over the indicated wavelength range and are also compared with resonant excitation from Figure 3.

Table S11. Lifetimes from Table S7 and S8 (670-750 nm) converted to rate constants in units of ps^{-1}. The differences in rate constants comparing solution and matrix samples are additionally calculated. In TPCb the difference can be attributed to the impact of cumulene twisting. In TPC the difference represents the role of phenyl rotation and cumulene twisting.

	TPC	**TPCb**
matrix	0.0013	0.059
solution	0.36	0.091
solution – matrix	0.36	0.032

In the TPCb matrix there is an intrinsic decay rate constant of 0.059 ps^{-1}, which accelerates by ~50% to 0.091 ps^{-1} in solution when cumulene twisting is enabled. Assuming all decay is nonradiative in these samples, and that the cumulene twisting is inactive in the matrix, the difference in rate constants of 0.032 ps^{-1} corresponds to the contribution that cumulene twisting makes to the overall decay constant in solution. To extend this analysis to TPC, we further assume that TPC exhibits a comparable decay rate constant associated with cumulene twisting. The solution-phase decay constant of 0.36 ps^{-1} then partitions into a cumulene twisting channel (0.032 ps^{-1}) and a phenyl rotation channel (0.33 ps^{-1}), revealing the latter to be by far the dominant decay pathway. The presence of this second channel and its suppression in the polymer matrix is responsible for the markedly larger change in decay rate between matrix and solution for TPC.

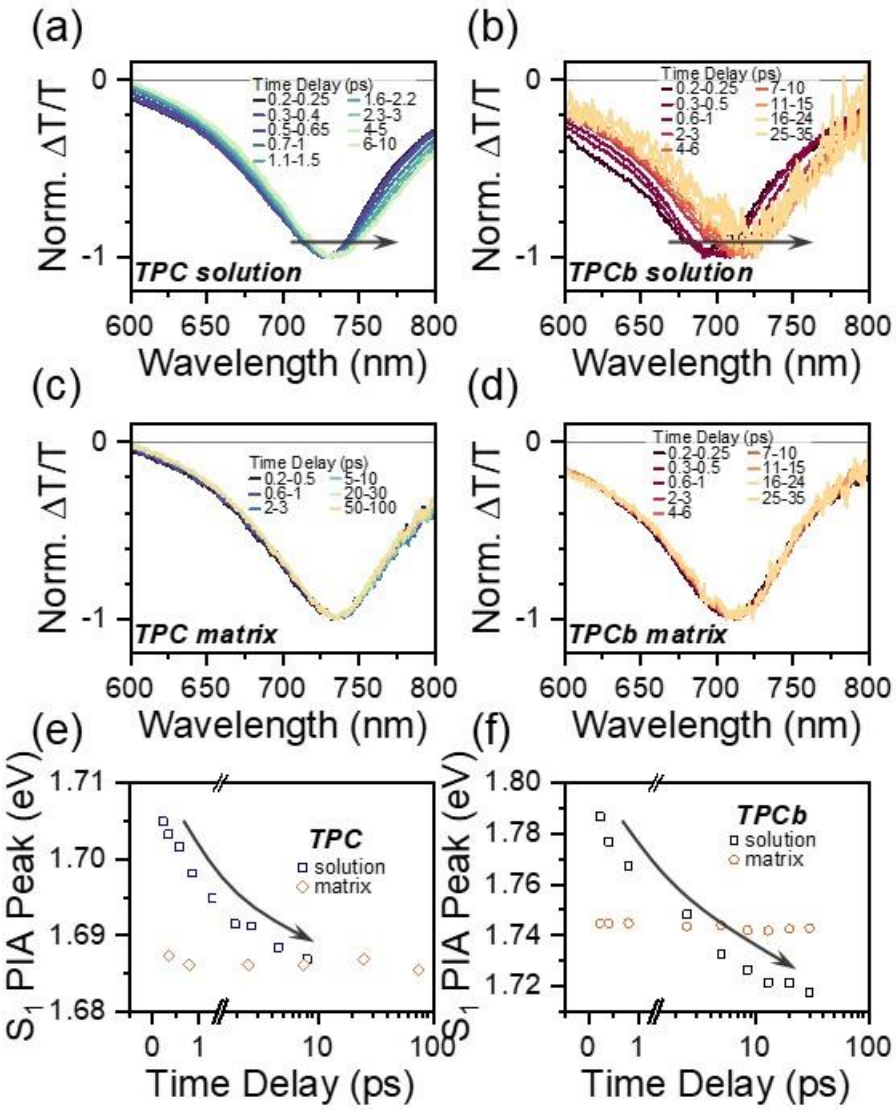

Figure S24. S_1 PIA peak position (converted to eV) tracked over time in both TPC and TPCb solutions and matrices. (a-d) show the same TA spectral slices from Figures 2 and 3 but normalized and zoomed to the S_1 PIA to show the spectral evolution. The extracted peak position from these spectra are shown in (e) and (f). Peak position was tracked out until the spectra decayed to noise.

In a solution of TPCb, phenyl torsion is nonexistent, so cumulene bond rotation should be the primary motion occurring in the excited state. In a matrix of TPCb, cumulene bond rotation will also become blocked. Thus, because we only observe a redshift of the S_1 PIA in the solutions of TPCb, we assign it to be caused by cumulene bond rotation. We see a similar but less pronounced redshift in TPC which indicates it is also related to cumulene bond rotation. The redshift continues for the full duration of the excited state lifetime in solution but is always

absent in the matrix samples. Recalling that the lifetime of TPCb is negligibly affected by environmental effects, this PIA redshift is the best tool to track cumulene bond rotation in these samples. Its slower evolution than the decay rate additionally supports the fact that cumulene bond rotation has no major impact on the quenching mechanism.

References

30. Connors, R.E.; Chynwat, V.; Clifton, C.H.; Coffin, T.L. Temperature Dependence of Aryl Butatriene Fluorescence: Barrier to Twisting on S 1 for 1,1,4,4-Tetraphenylbutatriene. *Journal of Molecular Structure* **1998**, *443*, 107–113, doi:10.1016/S0022-2860(97)00363-3.

45. Zang, Y.; Zou, Q.; Fu, T.; Ng, F.; Fowler, B.; Yang, J.; Li, H.; Steigerwald, M.L.; Nuckolls, C.; Venkataraman, L. Directing Isomerization Reactions of Cumulenes with Electric Fields. *Nat Commun* **2019**, *10*, 4482, doi:10.1038/s41467-019-12487-w.

47. Kerisit, N.; Gawel, P.; Levandowski, B.; Yang, Y.-F.; García-López, V.; Trapp, N.; Ruhlmann, L.; Boudon, C.; Houk, K.N.; Diederich, F. A Four-Step Synthesis of Substituted 5,11-Dicyano-6,12-Diaryltetracenes with Enhanced Stability and High Fluorescence Emission. *Chem. Eur. J.* **2018**, *24*, 159–168, doi:10.1002/chem.201703903.

48. Dahl, B.J.; Mills, N.S. Antiaromatic Spacer-Bridged Bisfluorenyl Dications Generated by Superacid Induced Ionization. *J. Am. Chem. Soc.* **2008**, *130*, 10179–10186, doi:10.1021/ja711501k.